Fluoropolymer/GAP Block Copolyurethane Binders: Sensitivity, Mechanical Properties and Reactive Properties with Aluminum

Minghui Xu (mhuixu@163.com)
Xi'an Modern Chemistry Research Institute
Xianming Lu
Xi'an Modern Chemistry Research Institute
Ning Liu
Xi'an Modern Chemistry Research Institute
Qian Zhang
Xi'an Modern Chemistry Research Institute
Hongchang Mo
Xi'an Modern Chemistry Research Institute
Zhongxue Ge
Xi'an Modern Chemistry Research Institute

Research Article

Keywords: olid propellant, energetic copolyurethane binder, PBFMO, drop weight test, XPS, tensile test, SEM, DSC

Posted Date: February 16th, 2021

DOI: https://doi.org/10.21203/rs.3.rs-199382/v1

Fluoropolymer/GAP block copolyurethane binders: Sensitivity, mechanical properties and reactive properties with aluminum

MinghuiXu,[a,b,*] Xianming Lu,[b] Ning Liu,[b] Qian Zhang,[b] Hongchang Mo,[b] and Zhongxue Ge[b]

[a] State Key Laboratory of Fluorine & Nitrogen Chemicals, Xi'an 710065 (P. R. China)

[b] Xi'an Modern Chemistry Research Institute, Xi'an 710065 (P. R. China)

Email: mhuixu@163.com

Abstract: In order to enhance the application properties of GAP in solid propellant, an energetic copolyurethane binder, (poly[3,3-bis(2,2,2-trifluoro-ethoxymethyl)oxetane] glycol-*block*-glycidylazide polymer (PBFMO-*b*-GAP) was developed. The PBFMO-*b*-GAP was prepared using poly[3,3-bis(2,2,2-trifluoro-ethoxymethyl)oxetane] glycol (PBFMO) which preparing from cationic polymerization and GAP as the raw materials, TDI as the coupling agent via a prepolymer process. The molecular structure of copolyurethane was confirmed by FT-IR, NMR, GPC. The impact sensitivity, mechanical properties and thermal behavior of PBFMO-*b*-GAP were studied by drop weight test, XPS, tensile test, SEM, DSC and TG/DTG respectively. The results proved that the introduction of fluoropolymer can evidently reduce the sensitivity of GAP based polyurethanes and enhance their mechanical behavior (the tensile strength up to 5.75MPa with a breaking elongation of 1660 %). Also, PBFMO-*b*-GAP exhibited an excellent resistance to thermal decomposition up to 200°C and good compatibility with Al and HMX. Cook-off test was used to investigate the reactive of copolyurethanes and Al, the results indicated that the copolyurethanes could react with Al efficiently and release significantly more heat. Therefore, the energetic copolyurethanes may serve as promising energetic binders for future propellant formulations.

1.Introduction

A recent trend in the field of energetic material formulations (explosives/propellants) is to replace inert binders (viz., HTPB, CTPB, HTPE, etc.) by energetic binders, which contain energetic groups

such as $-N_3$ (azide), nitro (C–nitro, O–nitro (nitrate ester), N–nitro (nitramine) and difluroamine groups, to impart additional energy to the system[1-3]. Among energetic polymers, glycidyl azide polymer (GAP) has been extensively studied as polymeric binders since it was first reported in a patent in 1972 by Vandenburg[4-6]. Due to its high density with positive heat of formation of +117.2 kcal mol^{-1}, high density (1.3g cm^{-3}), low glass-transition temperature (Tg=-45°C), good thermally stability, low detonation tendency, and also high burning rate ((1cm s^{-1} at 40 atmospheres)[7,8]. GAP has become the hotspot in the field of energy materials by offering a unique energetic binder and plasticizer system for advanced propellants and plastic bonded explosives (PBX) for achieving higher performance[9]. However, traditional GAP-based binders are thermosetpolymer and usually difficult to recycled. Moreover, it also suffers from high sensitive and inferior mechanical behavior which due to their highly polarity of azide groups and poor flexibility of polymer backbone[10].

In order to overcome these difficulties and also to obtain a better performance, various energetic polymeric binders have been developed in the last two decades. Energetic thermoplastic elastomers (ETPE) as high performance recyclable polymeric binders have received widespread attention in the past decades[11]. Generally, ETPE as a multiblock copolymer consists of hard segments and soft segments. Under room temperature, the hard segments, which act as fillers and physical crosslinks, are in a crystalline state or amorphous glassy state while the soft segments are in a rubbery state that leads to the flexibility. These polymers exhibit excellent mechanical and recyclable properties owing to the phase separation between hard and soft blocks and reversibly cross-linking points[12,13]. Thus, development of novel ETPE has attracted extensive attentions of many researchers in recent years[14,15].

In the past three decades, fluoropolymers have gained considerable attention in the energetic

material community (such as aerial infrared decoys, igniters, tracking flares, reactive binder systems, and solid fuel rocket propellants) as high explosive binders, owing to their high densities, long-term chemical stabilities, low coefficients of friction, and good compatibility with the main ingredients (oxidizers, metal fuels and plasticizer)[16-18]. Particularly, fluoropolymers can release high reaction energy due to their strong oxidation[19-21], for instance, the magnesium, Teflon, and Viton system (MTV) as one of the well-known compositions used in decoys and flares, can release especially large specific reaction energy of 9.4 kJ g^{-1}, in comparison with TNT and RDX yield just 3.72 kJ g^{-1} and 6.569 kJ g^{-1} , respectively[22]. Therefore, synthesis of fluorine-containing GAP based ETPE may be a promising method to improve its performance of application.

In this study, fluoropolymer/GAP block copolyurethane binders were synthesized via a prepolymer process by coupling together poly[3,3-bis(2,2,2-trifluoroethoxymethyl) oxetane] glycol (PBFMO) and GAP to decrease the sensitivity, enhance the mechanical properties and also promote the reactive efficiency with Al. The chemical structure and molecular weight of copolyurethanes were characterized by FTIR, NMR, GPC. The impact sensitivity and mechanical properties of the copolyurethanes were tested by drop weight test, XPS, tensile test and SEM respectively. The thermal properties of copolyurethanes and their compatibility with Al, HMX were also described by differential scanning calorimetry (DSC), thermal gravimetric analysis (TGA). The reactivity of PBFMO-*b*-GAP/Al complex was investigated by cook-off test.

2.Results and discussion

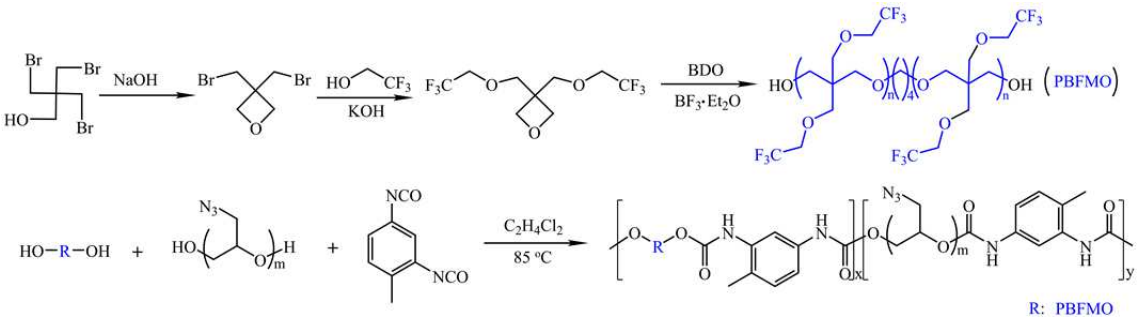

Scheme 1. The synthesis route of PBFMO-*b*-GAP copolyurethane

2.1 Preparation of PBFMO-b-GAP copolyurethane

The synthesis of PBFMO-*b*-GAP copolyurethane was done via a prepolymer process using PBFMO and GAP as the raw materials, TDI as the coupling agent, which was described in **Scheme 1.** The structure of the as-synthesized PBFMO-*b*-GAP was confirmed by FTIR and NMR. The IR spectra gave a first confirmation of the copolymer structure. As shown in **Figure 1**, the characteristic adsorption peak at 1276 cm^{-1} explained the $–CF_3$ stretching vibration of PBFMO, and the bands around 1135 cm^{-1} accounted for the C–O group stretching vibration of PBFMO[23,24]. The appearance of strong peak at 2093 cm^{-1} were attributed to $–N_3$ from GAP and the appearance of 3320 cm^{-1} was due to the –NH stretching vibration, the appearance of 1726 cm^{-1}, 1531 and 1376 cm^{-1} were assigned to C=O and –NH stretching bands of urethane group[25,26]. Therefore, such results gave strong evidence that the reaction of PBFMO with GAP indeed by the formation of PBFMO-*b*-GAP polyurethane.

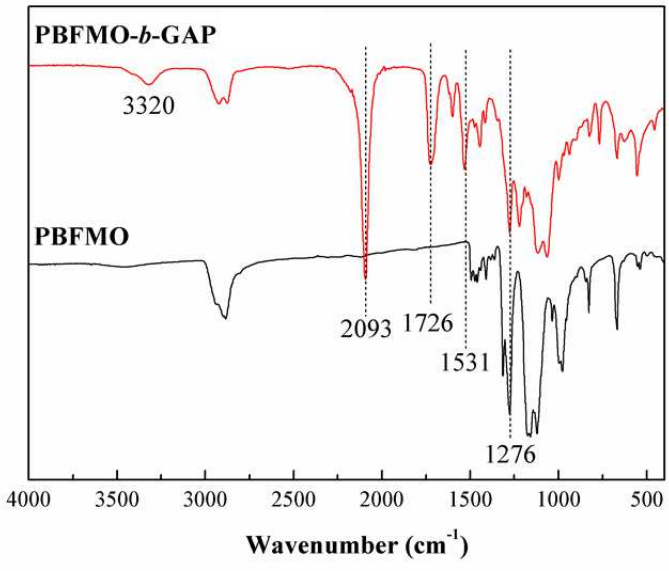

Figure 1. FTIR spectra of (A) PBFMO and (B) PBFMO-*b*-GAP copolyurethane.

As shown in **Figure 2A**, the signals of a broad band at 3.62 ppm attributed to methylene protons of GAP and PBFMO, and the peak appeared at 3.33 ppm was correspond to methylene protons of PBFMO side chain. The corresponding ^{13}C-NMR (**Figure 2B**) also indicated the presence of all the carbons in the GAP and PBFMO. The correspond carbons signals of methylene carbons from GAP and PBFMO appeared at 69.5 and 77.8 ppm. The signal for 51.6 ppm is attributed to the quaternary carbon atom of C–N_3[27]. The signal at 2.17 ppm belongs to methylene protons of the BDO which was the initiator of PBFMO and GAP, the corresponding carbon signals were appeared at 25.7 ppm. The signal at 1.77 ppm and 6.5-8 ppm were attributed to the methyl protons and methine protons on benzene rings of the TDI, respectively, and the corresponding carbons signals were appeared at 17.1 ppm and 120-135 ppm. Moreover, as shown in **Figure 2C** of ^{19}F NMR, the peak at -74.4 ppm was attributed to the –CF_3 of the side chain[28]. These signal positions observed in the NMR spectra of PBFMO-*b*-GAP strictly corroborated our FTIR analysis results.

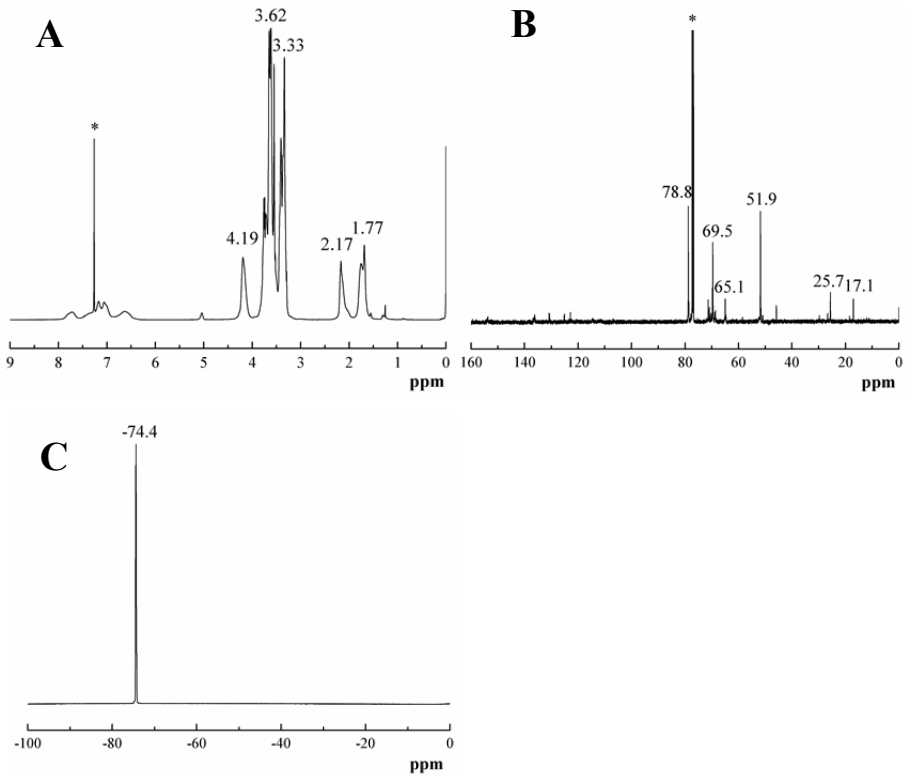

Figure 2. ^{1}H-NMR spectra (A),^{13}C-NMR spectra (B) and^{19}F-NMR spectra (C) of PBFMO-*b*-GAP in $CDCl_3$.

2.2 Density, Sensitivity and XPS of PBFMO-b-GAP copolyurethane

To investigate the different PBFMO-*b*-GAP copolyurethanes, the molar ratio of PBFMO/GAP was set at 1/3, 1/9 and 1/19, during chain coupling by TDI to obtain PBFMO-*b*-GAP-1$^{\#}$, 2$^{\#}$ and 3$^{\#}$ respectively. As showed in **Table 1**, the density of PBFMO-*b*-GAP was around 1.273~1.308 g cm^{-3}, which is higher than that of the control group (GAP based polyurethane, GAP-ETPE 1.263 g cm^{-3}). It is well known that polymers containing –CF_3 group increase its density, which is seen in the present study also[29]. The impact sensitivity of energetic polymer gels were characterized by the drop weight test, and the results are also showed in **Table 1**. It can be seen that the sensitivity of energetic materials is reduced with the mass ratio of polymer in the gel increases. Particularly noteworthy is the fact that the PBFMO/GAP molar ratio at 1/19 is markedly less sensitive than the pure GAP based polyurethane. Therefore, it appeared that the introduction of fluoropolymer may be manipulated to

reduce the sensitivity of very high energy composite energetic materials made in this fashion.

Table 1. Relative molecular mass, density and H_{50} of GAP based polyurethanes in different molar ratios

Sample	PBFMO/GAP molar ratio	M_n (10^3gmol^{-1})	Density (g cm^{-3})	H_{50} (cm)
PBFMO-*b*-GAP-1$^{\#}$	1/3	33	1.308	>129
PBFMO-*b*-GAP-2$^{\#}$	1/9	31	1.290	>129
PBFMO-*b*-GAP-3$^{\#}$	1/19	30	1.273	56.2
GAP-ETPE	0	32	1.263	9.55

XPS was employed to detect the change of elementary composition on the elastomers surface, and provide valuable insight into the influence between sensitivity and fluorine content[30]. The N1s, C1s, O1s and F1s elements of XPS spectra of elastomers surface and its surface compositions expressed quantitatively as atomic weight percentages are summarized in **Figure 3**and **Table 2**, respectively. Due to the introduction of different content of PBFMO, the concentrations of F from elastomers surface increase from 0 to 13.05%, meanwhile the atomic weight percentage of N decrease from 12.16% to 1.54%. The results indicated that the increase of the F elements of the surface may decrease of the coefficients of friction of the atomic weight percentage and decrease its sensitivity.

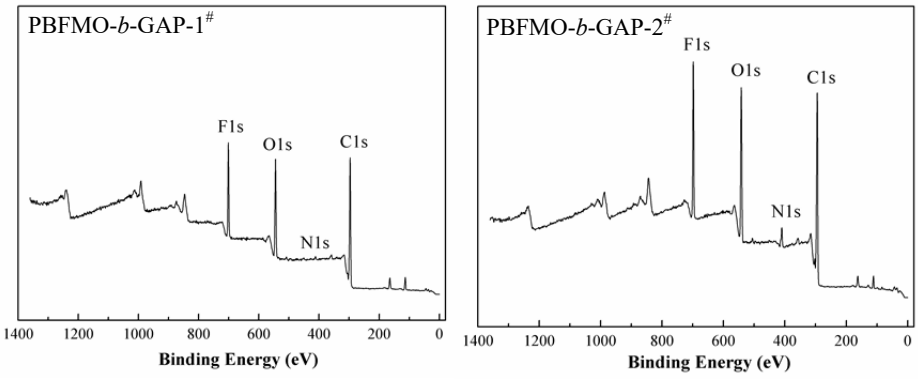

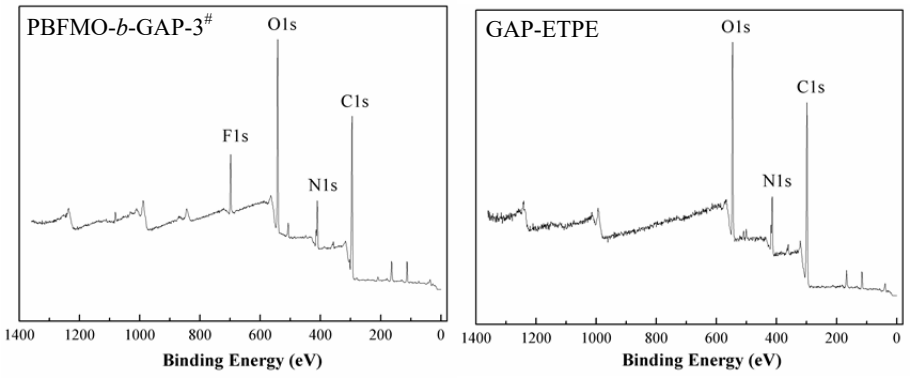

Figure 3. XPS curves of the gels prepared from GAP based polyurethanes

Table 2. Atomic weight percentages of XPS cruves

Sample	C (%)	O (%)	N (%)	F (%)
PBFMO-*b*-GAP-1#	65.22	20.18	1.54	13.05
PBFMO-*b*-GAP-2#	63.00	19.76	4.33	12.91
PBFMO-*b*-GAP-3#	60.88	23.42	10.36	5.34
GAP-ETPE	63.8	24.04	12.16	0

2.3 Mechanical Properties of PBFMO-b-GAP copolyurethane

Mechanical properties of the PBFMO-*b*-GAP copolyurethanes prepared from various ratio of PBFMO/GAP prepolymers were evaluated with the universal testing machine as shown in **Figure 4**. An overlay of stress-strain curves of PBFMO-*b*-GAP copolyurethanes shown in **Figure 4**, showed an initial linear deformation, subsequent extension and ultimately lead to the failure. It is clearly that the tensile strength of PBFMO-*b*-GAP increase from 2.9 to 5.75 MPa along with the increase of PBFMO content, meanwhile the elongation at break decrease from 2056% to 1660%. In general, the crosslinking density is a dominant factor to determining mechanical performances for network-structured materials, higher crosslinking density results in higher tensile strength and Young's modulus, and lower elongation at break. In this work, PBFMO works as a hard segment in

PBFMO-*b*-GAP copolyurethanes, under room temperature, it aggregate with each other to form physical cross-linking points. The results reveal that the PBFMO could be competent for hard segment in GAP based polyurethanes to increase their mechanical behavior.

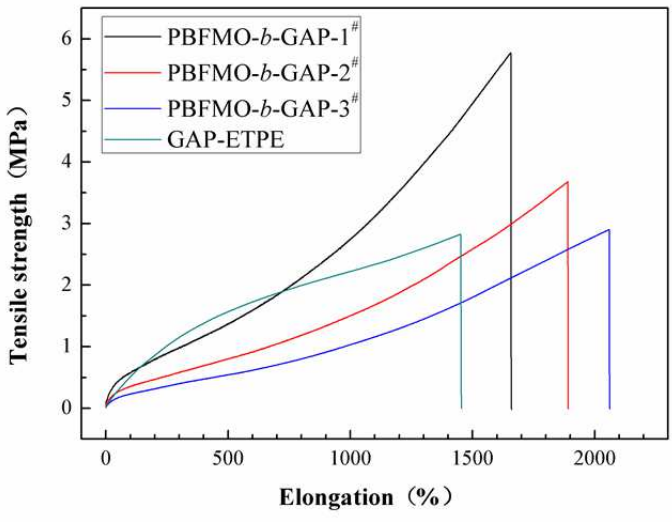

Figure 4. Tensile testing of polymer samples prepared from PBFMO-*b*-GAP copolyurethane.

To get some insight of the observed enhancement of the mechanical properties of the PBFMO-*b*-GAP copolyurethane, the fractured surfaces of the elastomers films with various molar ratio of GAP/PBFMO were studied by SEM. As shown in **Figure 5**, with an increase in the molar ratio of GAP/PBFMO, the wrinkle and ravines of the fractured surfaces were more and more obvious while the fractured stripes became deeper. It is well known that phase separation exists between the soft and hard segments, and the hard segments aggregate with each other to form physical cross-linking points throughout the soft segments, resulting in good mechanical properties. The phenomenon might be ascribed to the fact that structural heterogeneity in the films gradually aggravated with an increase of crosslinking densities. It may reveal that the introduction of PBFMO uniformly improved the phase separation of gel prepared from PBFMO-*b*-GAP, and resulted in good mechanical properties[31]. Consideration of PBFMO-*b*-GAP-1$^{\#}$ which possessing the best tensile strength and sufficient elongation at break, was selected in the next experiment.

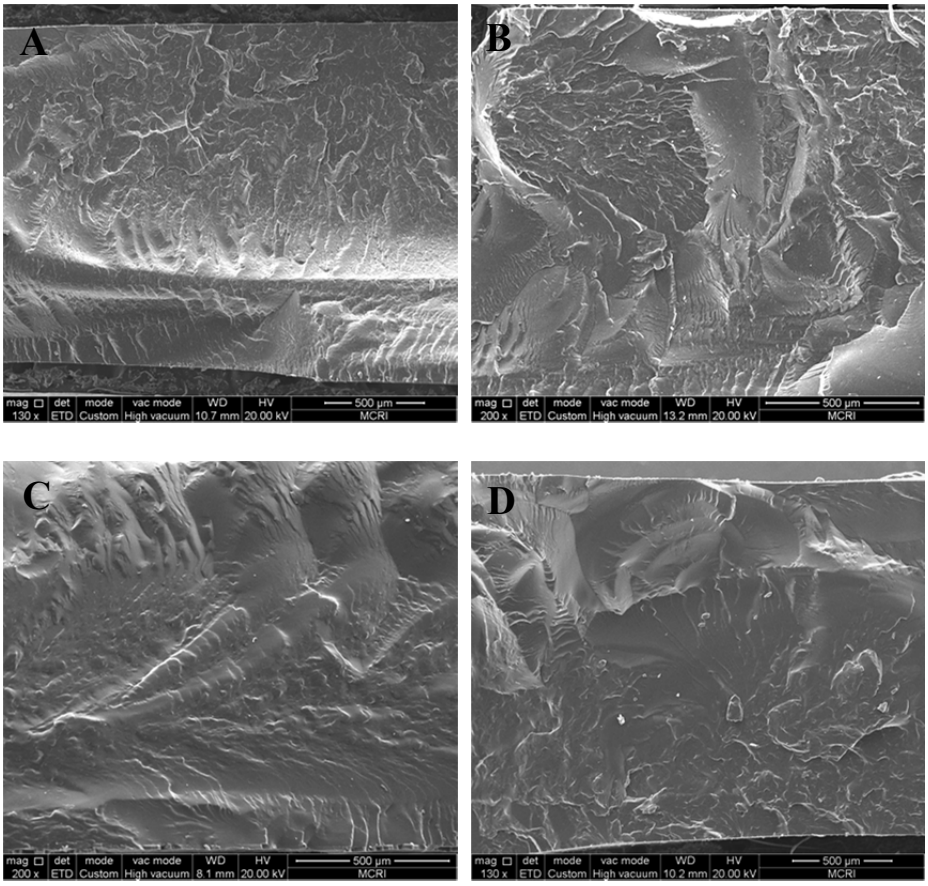

Figure 5. SEM images for the fracture surface of the gels prepared from (A) PBFMO-*b*-GAP-1[#], (B) PBFMO-*b*-GAP-2[#], (C) PBFMO-*b*-GAP-3[#] and (D) GAP-ETPE.

2.4 Thermal decomposition

It is well known that the thermal stability of energetic binders plays an important role in the preparation, processing, storage, and application of energetic material[32,33]. Thus, DSC and TGA were applied to study the thermal decomposition behavior of PBFMO-*b*-GAP copolyurethane. The DSC curve of the PBFMO-*b*-GAP is presented in **Figure 6**, and the DSC curve of PBFMO-*b*-GAP showed four exothermic peaks. The first exothermic peak at 40 °C was the melting point of PBFMO, the second exothermic peak at 247 °C was caused by the decomposition of side chain azide groups on PBFMO-*b*-GAP to give nitrogen molecules, and the other two peaks at 453 and 504 °C were due to PBFMO-*b*-GAP main chain decomposition. The TGA and DTG traces of PBFMO-*b*-GAP were

showed in **Figure 7**, and display two distinct regions of weight loss. The first sharp weight loss of around 25% with respect to the total was at 246 °C, which was corresponding to the stripping of the azide groups of the side chain which in correspondence of the same phenomena of DSC. It is seen from the TGA curve that after the sharp step does not level and shows a gradual weight loss. The phenomenon is superposed to an incipient degradation of the polymer chains. In any case, both DSC and TGA confirm that the PBFMO-*b*-GAP start to decompose/degrade at high temperature, thus showing a satisfactory thermal stability.

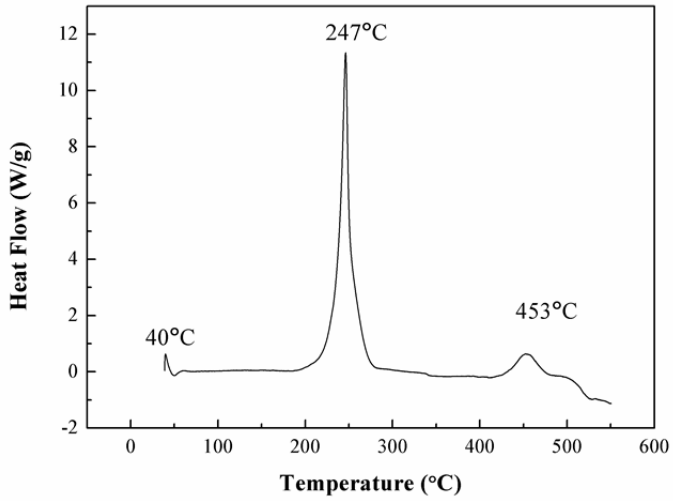

Figure 6. DSC curve of PBFMO-*b*-GAP copolyurethane.

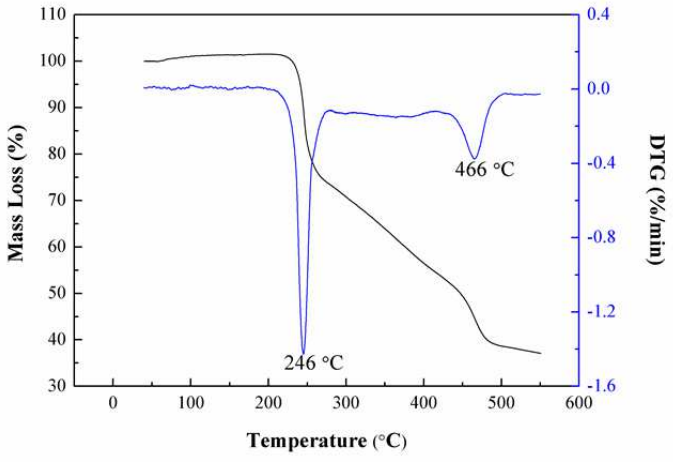

Figure 7. TG/DTG curves of PBFMO-*b*-GAP copolyurethane.

2.5 Compatibility testing

Compatibility is an important safety and reliability index used to evaluate the production, application and storage of energetic materials[34,35]. Usually, compatibility can be evaluated from DSC curves by studying the effect of the contact material on the exothermic decomposition temperature of the explosives. In this study, DSC curves were used to determine the compatibility of PBFMO-*b*-GAP with the main energetic components, such as HMX and Al. Typical DSC curves of binary systems PBFMO-*b*-GAP/HMX, PBFMO-*b*-GAP/Al were shown in **Figure 8**. According to the standards of compatibility, the binary systems PBFMO-*b*-GAP/HMX and PBFMO-*b*-GAP /Al had good compatibilities because their ΔTp values were all less than 2 °C. It indicated that PBFMO-*b*-GAP could be safely used in HMX based propellant.

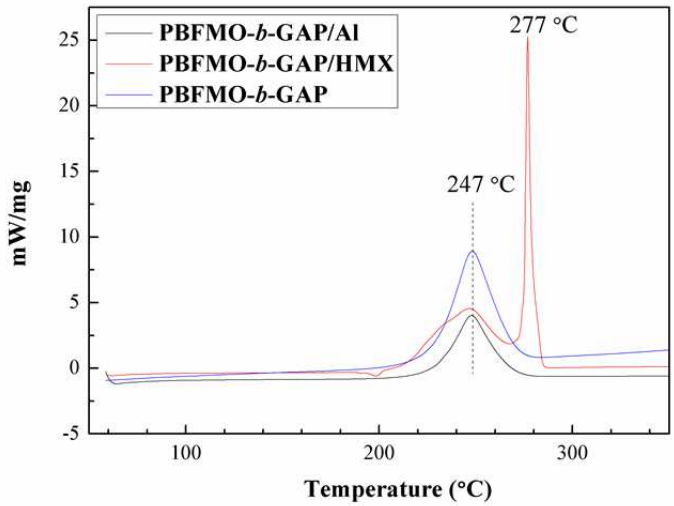

Figure 8. DSC curves of PBFMO-*b*-GAP, PBFMO-*b*-GAP/HMX complex and PBFMO-*b*-GAP/Al complex.

2.6 Cook-off test

The cook-off experiments were used to study the thermal performance of PBFMO-*b*-GAP and Al[36-38]. As shown in **Figure 9**, the cook-off curves showed initial linear calefactive and impetuously calefactive ultimately lead to linear calefactive again. The impetuously calefactive of inner

temperature can be contribute to the samples start to exothermic decomposition, the release gas reactive with Al and give more exothermal. Generally, the integral of outer and inner temperature curves can evaluate the heat release due to the reaction between elastomers and Al. In this work, the integral of PBFMO-*b*-GAP/Al compositions showed a remarkable increase than the control group. It implied that the PBFMO-*b*-GAP can efficiently react with Al and release significantly more heat[39].

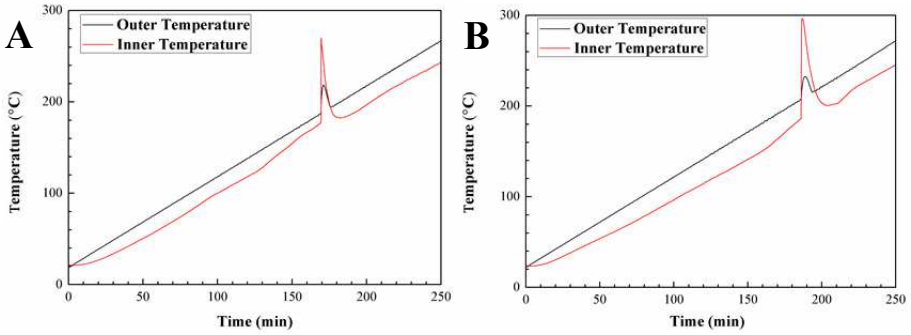

Figure 9. Cook-off curves of GAP-ETPE/Al (A) and PBFMO-*b*-GAP/Al (B)

3.Conclusions

In conclusions, a copolyurethane binder, PBFMO-*b*-GAP, was synthesized on GAP as a soft segment and TDI extended PBFMO as hard segment. From FT-IR, NMR, and GPC results, the PBFMO-*b*-GAP was synthesized successfully via a prepolymer process. The drop weight test and XPS results indicated that the introduction of fluoropolymer can evidently reduce the sensitivity of PBFMO-*b*-GAP polyurethane. The PBFMO-*b*-GAP showed an enhanced tensile strength of 5.75 MPa with a breaking elongation of 1660%, and the tensile strength of PBFMO-*b*-GAP films increased with an increase of the PBFMO content. The DSC and TGA-DTG curves indicated that PBFMO-*b*-GAP have adequate resistance to thermal decomposition up to 200°C and begin to decompose gradually at about 230°C, and also have a good compatibility with Al and HMX. Cook-off results implied the PBFMO-*b*-GAP can effectively react with Al and release relatively

more quantity of heat. All these results indicated that PBFMO-*b*-GAP might serve as a potential energetic binder in propellant formulations.

4. Methods

Materials GAP with molecular weight of 3500 g mol^{-1} and hydroxy value of 0.9% was provided from the Liming Chemical Engineering Research and Design Institute of Luoyang. 2,2,2-trifluoroethanol, 2,2-bisbromomethyl-3-bromo-propan-1-ol, butane diol (BDO), BF_3-etherate and dibutyltindilaurate (DBTDL) were purchased from J&K scientific Ltd. (Shanghai). Toluene diisocyanate (TDI), N,N-dimethylformamide (DMF), dichloromethane (DCM) and ethanol were supplied by Chengdu Kelong Chemical Reagents Company. 1,2-dichloroethane was obtained from Chengdu Jinshan Chemical Reagent Company. BDO and BF_3-dimethyl ether were distilled under reduced pressure prior to use. All solvents for the reactions were analytical grade and were dried before use.

Synthesis of [3,3-bis(2,2,2-trifluoroethoxymethyl)oxetane] glycol (BFMO) As shown in **Scheme 1**, BFMO was synthesized according to the literature procedure in two steps[40]. First step was the synthesis of 3,3-bisbromomethyloxetane (BBMO). A mixture of 2,2-bisbromomethyl-3-bromo-propan-1-ol, NaOH, TBAB and DCM was stirred at 40 °C for 8 h. And then, the organic layer was separated, died with $MgSO_4$, and concentrated at atmospheric pressure to remove DCM. The residue was distilled under reduce pressure and the fraction of 94°C/4 mmHg was collected to give the purified BBMO as a colorless liquid (yield, 70%). Second step was the conversion of BBMO to BFMO, a typical compound synthesis are described below. BBMO, 2,2,2-trifluoroethanol, KOH and phase-transfer catalyst TBAB were charged into 100 mL three-necked round-bottom flask. The reaction mixture was stirred at 85 °C for 24 h. After the

reaction, the organic phase was separated, washed with distilled water and died over anhydrous $MgSO_4$. The BFMO was obtained by distillation and the fraction of 86 °C/4 mm Hg was collected (yield, 81.6%).

Polymerization of PBFMO The PBFMO was synthesized through cationic ring-opening polymerization of BFMO. A typical reaction procedure was as follows: BDO, BF_3-etherate and dried methylene chloride were charged into a three necked flask fitted with a thermometer under argon and left stirred for 1 h. BFMO was added into the mixture drop by drop within a period of 8 h, and the reaction mixture was then left under stirred for an additional 24 h. After then, the reaction was stopped by the addition of 1% sodium bicarbonate solution. The organic phase was washed with distilled water and concentrated by vacuum evaporation to acquire a white, wax polymer PBFMO (yield, 92.4%).GPC analysis: M_n= 6840 g mol^{-1}, PDI=1.22 (polystyrene standards).

Synthesis of PBFMO-b-GAP copolyurethane PBFMO-*b*-GAP copolyurethane was synthesized via a prepolymer process using PBFMO and GAP as raw materials, TDI as coupling agent. A typical reaction procedure was as follows: Exactly GAP, PBFMO, and freshly distilled 1,2-dichloroethane were placed in a 250 mL four-neck flask equipped with a condenser, mechanical stirrer and thermometer under high purity argon (99.99%) and then heated to 60°C. TDI and DBTDL was then dissolved in 20 mL 1,2-dichloroethane and added dropwise into the reaction solution. After stirring for an additional 2 h, the reaction mixture was poured into 400 mL ethanol. The polymer was precipitated and separated out, dried in vacuum at 50°C for 24 h to obtain PBFMO-*b*-GAP copolyurethane (yield, 97%).

Measurements FTIR spectra were measured on a Bruker Tensor 27 instrument (KBr pellet) in the range of 4000–400 cm^{-1}. Nuclear magnetic resonance (NMR) spectra were recorded on a Bruker 500

MHz instrument with $CDCl_3$ as the solvent and tetramethylsilane as the internal standard. GPC was conducted on a Waters GPC, using tetrahydrofuran and polystyrene standards as the mobile phase and for calibration, respectively. A method of drop hammer impact sensitivity test for big-bill explosive was developed. The weight of the hammer was 5 kg and the drop height was between 0 ~ 1.29 m. The size of big-bill explosive was φ20 mm × 5 mm and its weight was 2.8 g. XPS analysis was performed using a Sigmaprobe instrument (ThermoElectron Corp., UK) equipped with a nonmonochromatic Al KR (hv =1486.6eV) source at a power of 300W. Mechanical properties of all the elastomers films were measured on an AG-X Plus testing machine (Shimadzu, Japan) with a tensile rate of 50 mm min^{-1}. The testing films were cut into strips with a width of 10 mm and a distance between testing marks was 30 mm, and kept at 0% humidity for 7 days before measurement. A mean value of five replicates from each film was taken. SEM observation was carried out on a VEGA 3 LMU scanning electron microscope (TESCAN, Czech Republic). All the elastomers films were frozen in liquid nitrogen, snapped and sputtered with gold until photographed. Differential scanning calorimetry (DSC) equipped with a TA instruments DSC Q1000 and Thermogravimetric analysis (TGA) equipped with a SDT Q600 TGA instrument (TA Instruments) were used to thermally characterize the samples, which were ramped between 25 and 500°C at a heating rate of 10°C min^{-1}.

The special equipment for slow cook-off test used in the research was designed by Institute of Chemical Materials, and its schematic diagram was shown in **Scheme 2.** The equipment has a power of 1500 W, and the heating rate of the heating cartridge wall was set at 1 °C min^{-1}, and the temperature range from the room temperature to 250 °C. In the slow cook-off test, we put PBFMO-*b*-GAP/Al complex samples hemisphere in test set-up and heated by the electric heating

cord, meanwhile the equal heating components of PBFMO-*b*-GAP was heated with an intelligent temperature controller to adjust the heating rate. Samples were well sealed, and the thermocouples were utilized to obtain their temperature vs time curves. Those experimental results were synthetically analyzed to the reactivity of the PBFMO-*b*-GAP/Al complex under slow heating stimulation.

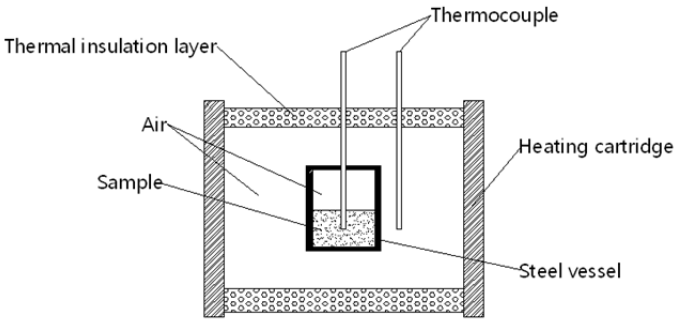

Scheme 2. Schematic geometry of cook-off test

References

1. Cheng, T. Review of novel energetic polymers and binders - high energy propellant ingredients for the new space race. *Des. Monomers Polym.* **22** 1, 54-65 (2019).

2. Bodaghi, A. & Shahidzadeh, M. Synthesis and characterization of new PGN based reactive oligomeric plasticizers for glycidyl azide polymer. *Propellants Explos. Pyrotech.* **43** 4, 364-370 (2018).

3. Wang, Q., Wang, L., Zhang, X. & Mi, Z. Thermal stability and kinetic of decomposition of nitrated HTPB. *J. Hazard. Mater.* **172** 2-3, 1659-1664 (2009).

4. Hafner, S., Keicher, T. & Klapoetke, T. M. Copolymers based on GAP and 1,2-Epoxyhexane as Promising Prepolymers for Energetic Binder Systems. *Propellants Explos. Pyrotech.* **43** 2, 126-135 (2018).

5. Boopathi, S. K., Hadjichristidis, N., Gnanou, Y. & Feng, X. Direct access to polyglycidyl azide.and its copolymers

through anionic co-)polymerization of glycidyl azide. *Nat. Commun.* **10**, 293-301 (2019).

6. Frankel, M. B., Grant, L. R. & Flanagan, J. E. Historical development of glycidyl azide polymer. *Journal of J. Propul. Power* **8** 3, 560-563 (1992).

7. Murali Mohan, Y., Mani, Y. & Mohana Raju, K. Synthesis of azido polymers as potential energetic propellent binders. *Des. Monomers Polym.* **9** 3, 201-36 (2006).

8. Selim, K., Ozkar, S. & Yilmaz, L. Thermal characterization of glycidyl azide polymer GAP.and GAP-based binders for composite propellants. *J. Appl. Polym. Sci.* **77** 3, 538-546 (2000).

9. Gaur, B., Lochab, B., Choudhary, V. & Varma, I. K. Azido polymers - Energetic binders for solid rocket propellants. *J. Macromol. Sci., Polym. Rev.* **C43** 4, 505-545 (2003).

10. Ding, Y., Hu, C., Guo, X., Che, Y. & Huang, J. Structure and mechanical properties of novel composites based on glycidyl azide polymer and propargyl-terminated polybutadiene as potential binder of solid propellant. *J. Appl. Polym. Sci.* **131** 7, 40007-40014 (2014).

11. Sikder, A. K. & Reddy, S. Review on energetic thermoplastic elastomers ETPEs.for military science. *Propellants Explos. Pyrotech.* **38** 1, 14-28 (2013).

12. Yanagisawa, Y., Nan, Y., Okuro, K. & Aida, T. Mechanically robust, readily repairable polymers via tailored noncovalent cross-linking. *Science* **359** 6371, 72-80 (2018).

13. Hu, Y., Jian, X., Xiao, L. & Zhou, W. Microphase separation and mechanical performance of thermoplastic elastomers based on polyglycidyl azide)/polyoxytetramethylene glycol). *Polym. Eng. Sci.* **58**, 167-173 (2018).

14. Wang, G. & Luo, Y. Characterization of PBAMO/AMMO.ETPE prepared using different diisocyanates. *Propellants Explos. Pyrotech.* **41** 5, 850-854 (2016).

15. Zhang, Z. et al. Synthesis and characterization of novel energetic thermoplastic elastomers based on glycidyl azide polymer GAP.with bonding functions. *Polym. Bull.* **72** 8, 1835-1847 (2015).

16. Lee, I., Reed, R. R., Brady, V. L. & Finnegan, S. A. Energy release in the reaction of metal powders with fluorine containing polymers. *J. Therm. Anal.* **49** 3, 1699-1705 (1997).

17. Lee, J. H., Kim, S. J., Park, J. S. & Kim, J. H. Energetic Al/Fe2O3/PVDF composites for high energy release: Importance of polymer binder and interface. *J. Therm. Anal.* **24** 10, 909-914 (2016).

18. Dattelbaum, D. M. et al. Equation of state and high pressure properties of a fluorinated terpolymer: THV 500. *J. Appl. Phys.* **104** 11, 113525-113535 (2008).

19. McCollum, J., Pantoya, M. L. & Iacono, S. T. Activating aluminum reactivity with fluoropolymer coatings for improved energetic composite combustion. *ACS Appl. Mater. Interfaces* **7** 33, 18742-18749 (2015).

20. Gong, F. et al. Highly thermal stable TATB-based aluminized explosives realizing optimized balance between thermal stability and detonation performance. *Propellants Explos. Pyrotech.* **42** 12, 1424-1430 (2017).

21. Yang, H., Huang, C. & Chen, H. Tuning reactivity of nanoaluminum with fluoropolymer via electrospray deposition. *J. Therm. Anal. Calorim.* **127** 3, 2293-2299 (2017).

22. Rider, K. B., Little, B. K., Emery, S. B. & Lindsay, C. M. Thermal analysis of magnesium/perfluoropolyether pyrolants. *Propellants Explos. Pyrotech.* **38** 3, 433-440 (2013).

23. Wang, X., Hu, J., Li, Y., Zhang, J. & Ding, Y. The surface properties and corrosion resistance of fluorinated polyurethane coatings. *J. Fluorine Chem.* **176**, 14-19 (2015).

24. Liu, X. et al. Synthesis of perfluorinated ionomers and their anion exchange membranes. *J. Membr. Sci.* **515**, 268-276 (2016).

25. Tanver, A. et al. Energetic hybrid polymer network EHPN.through facile sequential polyurethane curation based on the reactivity differences between glycidyl azide polymer and hydroxyl terminated polybutadiene. *RSC Adv.* **6** 13, 11032-11039 (2016).

26. Ma, M. & Kwon, Y. Reactive cycloalkane plasticizers covalently linked to energetic polyurethane binders via facile

335 control of an in situ Cu-free azide-alkyne 1,3-dipolar cycloaddition reaction. *Polym. Chem.* **9** 45, 5452-5461 (2018).
336 27. Jin, B. et al. Synthesis, characterization, thermal stability and sensitivity properties of new energetic
337 polymers-PVTNP-g-GAPs crosslinked polymers. *Polymers* **8** 1, 10-23 (2016).
338 28. Shmatova, O. I. & Nenajdenko, V. G. Tetrazole-substituted five, six, and seven-membered cyclic amines bearing
339 perfluoroalkyl groups - efficient synthesis by azido-ugi reaction. *Eur. J. Org. Chem.* **2013** 28, 6397-6403 (2013).
340 29. Sarangapani, R., Reddy, S. T. & Sikder, A. K. Molecular dynamics simulations to calculate glass transition
341 temperature and elastic constants of novel polyethers. *J. Mol. Graphics Modell.* **57**, 114-121 (2015).
342 30. Cai, T., Yang, W. J., Neoh, K. G. & Kang, E. T. Polyvinylidene fluoride.membranes with hyperbranched antifouling
343 and antibacterial polymer brushes. *Ind. Eng. Chem. Res.* **51** 49, 15962-15973 (2012).
344 31. Malkappa, K. & Jana, T. Simultaneous improvement of tensile strength and elongation: An unprecedented
345 observation in the case of hydroxyl terminated polybutadiene polyurethanes. *Ind. Eng. Chem. Res.* **52** 36,
346 12887-12896 (2013).
347 32. Landsem, E. et al. Isocyanate-free and dual curing of smokeless composite rocket propellants. *Propellants Explos.*
348 *Pyrotech.* **38** 1, 75-86 (2013).
349 33. You, J. S., Kweon, J. O., Kang, S. C. & Noh, S. T. A kinetic study of thermal decomposition of glycidyl azide
350 polymer GAP)-based energetic thermoplastic polyurethanes. *Macromol. Res.* **18** 12, 1226-1232 (2010).
351 34. Pei, J. F. et al. Compatibility study of BAMO-GAP copolymer with some energetic materials. *J. Therm. Anal.*
352 *Calorim.* **124** 3, 1301-1307 (2016).
353 35. Li, Y., Li, J., Ma, S. & Luo, Y. Compatibility, mechanical and thermal properties of GAP/PEO-co-THF.blends
354 obtained upon a urethane-curing reaction. *Polym. Bull.* **74** 11, 4607-4618 (2017).
355 36. Ding, X. Y., Shu, Y. J., Xu, H. T. & Chen, Z. Q. Study on thermal behaviour of AP/LiBH4 energetic system.
356 *Propellants Explos. Pyrotech.* **43** 3, 267-273 (2018).

357 37. Li, W. F., Yu, Y. G., Ye, R. & Yang, H. W. Three-dimensional simulation of base bleed unit with AP/HTPB propellant
358 in fast cook-off conditions. *J. Energ. Mater.* **35** 3, 265-275 (2017).
359 38. Chen, L., Ma, X., Lu, F. & Wu, J. Y. Investigation of the cook-off processes of hmx-based mixed explosives. *Cent.*
360 *Eur. J. Energ. Mat.* **11** 2, 199-218 (2014).
361 39. Xu, M. et al. Fluorinated glycidyl azide polymers as potential energetic binders. *RSC Adv.* **7** 75, 47271-47278
362 (2017).
363 40. Jiang, W. C., Huang, Y. G., Gu, G. T., Meng, W. D. & Qing, F. L. A novel waterborne polyurethane containing short
364 fluoroalkyl chains: Synthesis, characterization and its application on cotton fabrics surface. *Appl. Surf. Sci.* **253** 4,
365 2304-2309 (2006).

366 Acknowledgements

367 The authors gratefully acknowledge the financial support from the China Postdoctoral
368 Science Foundation (2016M592851).

369 Author contributions

370 Conceptualization, M.X. and X.L.; Methodology, M.X., X.L. and H.M.; Investigation, M.X.;
371 Resources, X.L. Q.Z. and H.M.; Writing—original draft preparation, M.X.; Writing—review and
372 editing, M.X., Q.Z. and H.M.; Supervision, M.X., N.L. and Z.G.; Funding acquisition, M.X.

373 Competing interests

374 The authors declare no competing interests.

375

Figures

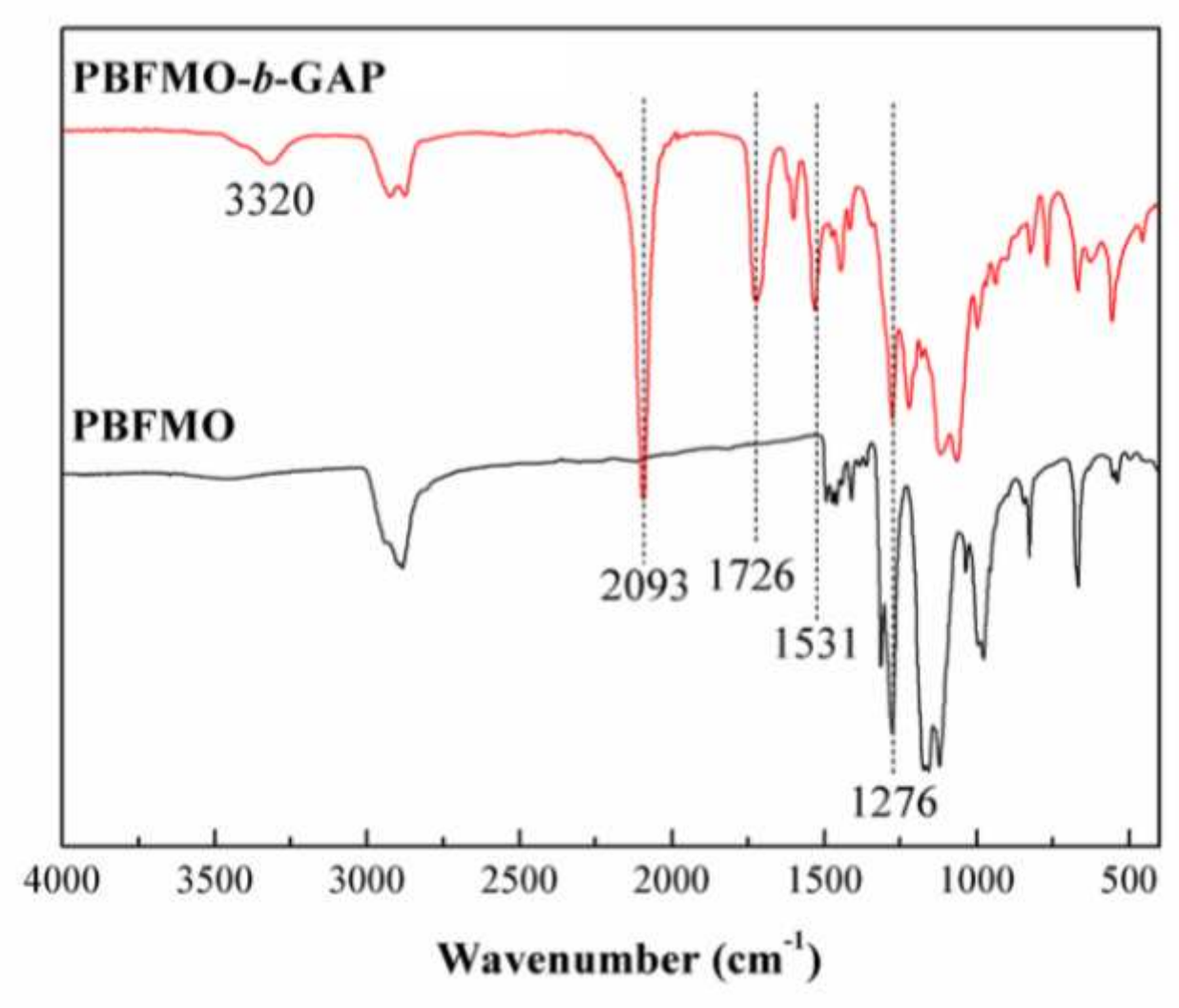

Figure 1

FTIR spectra of (A) PBFMO and (B) PBFMO-b-GAP copolyurethane.

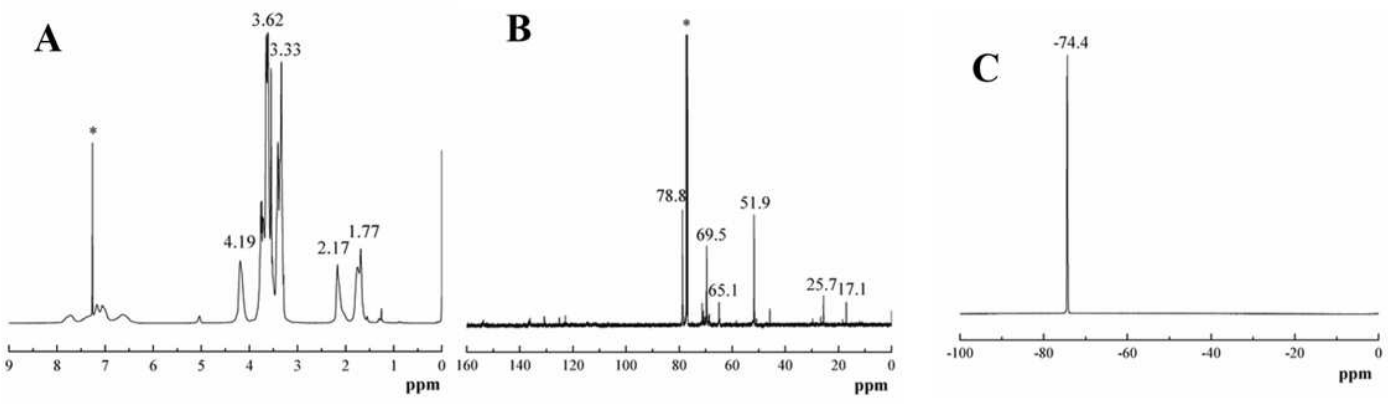

Figure 2

H-NMR spectra (A),13C-NMR spectra (B) and19F-NMR spectra (C) of PBFMO-b-GAP in CDCl3.

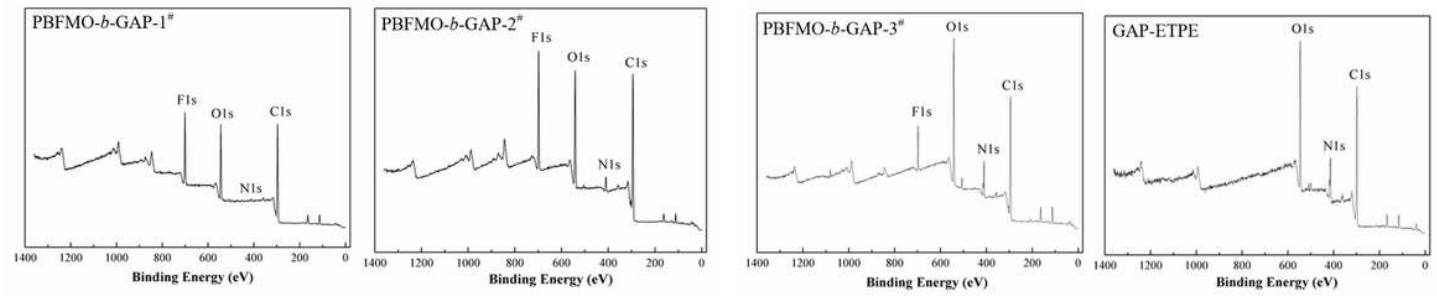

Figure 3

XPS curves of the gels prepared from GAP based polyurethanes

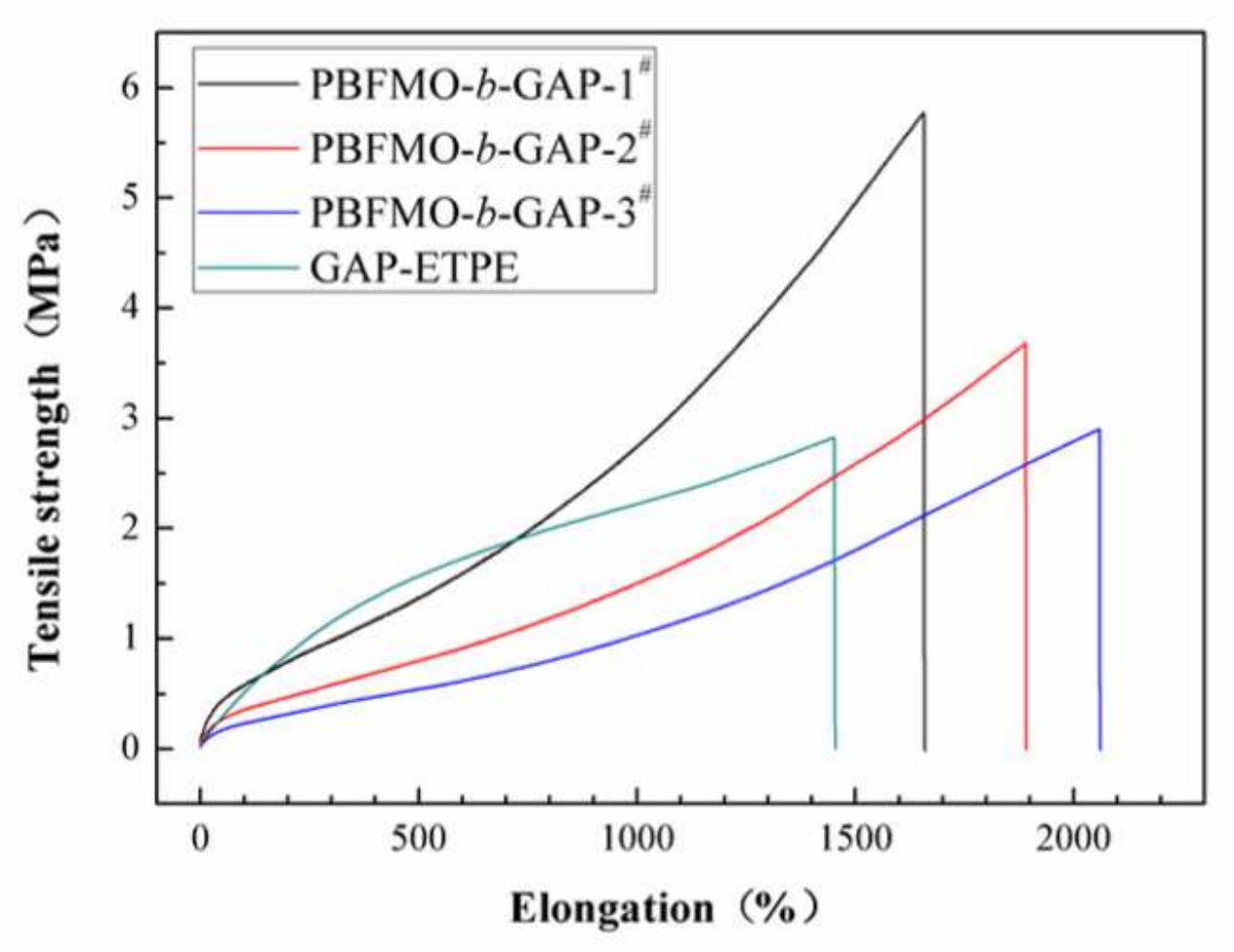

Figure 4

Tensile testing of polymer samples prepared from PBFMO-b-GAP copolyurethane.

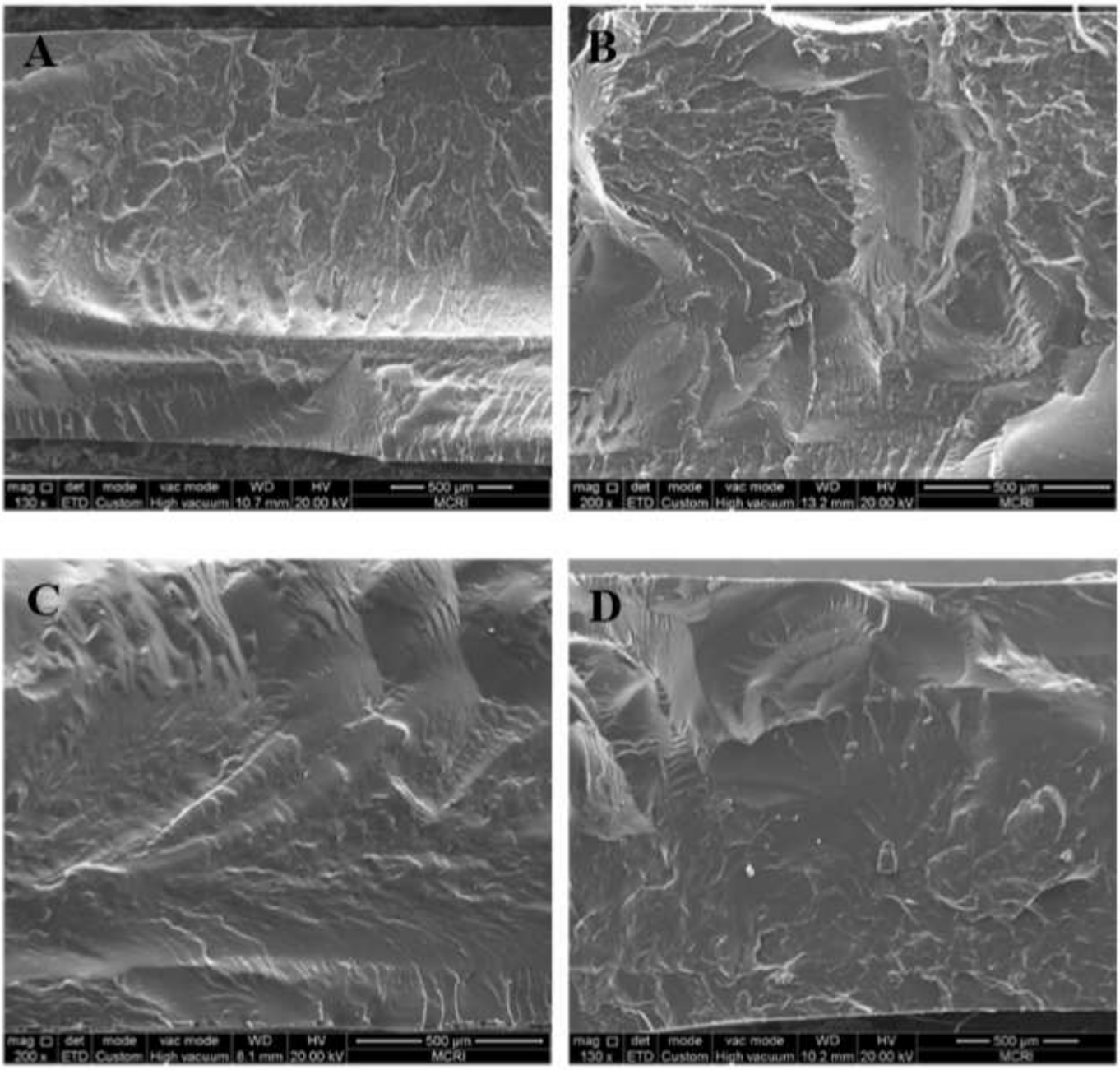

Figure 5

SEM images for the fracture surface of the gels prepared from (A) PBFMO-b-GAP-1#, (B) 150 PBFMO-b-GAP-2#, (C) PBFMO-b-GAP-3# and (D) GAP-ETPE.

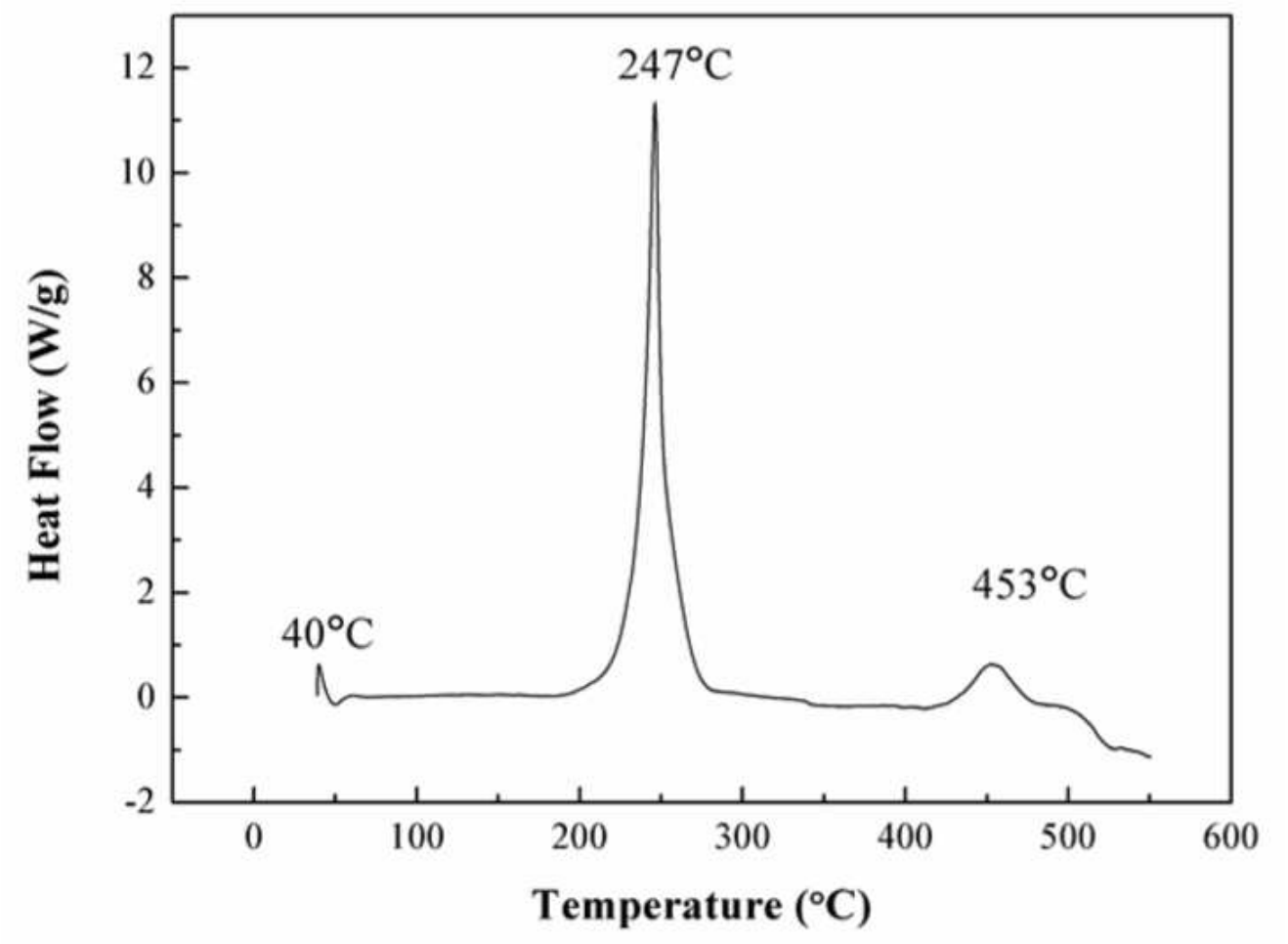

Figure 6

DSC curve of PBFMO-b-GAP copolyurethane.

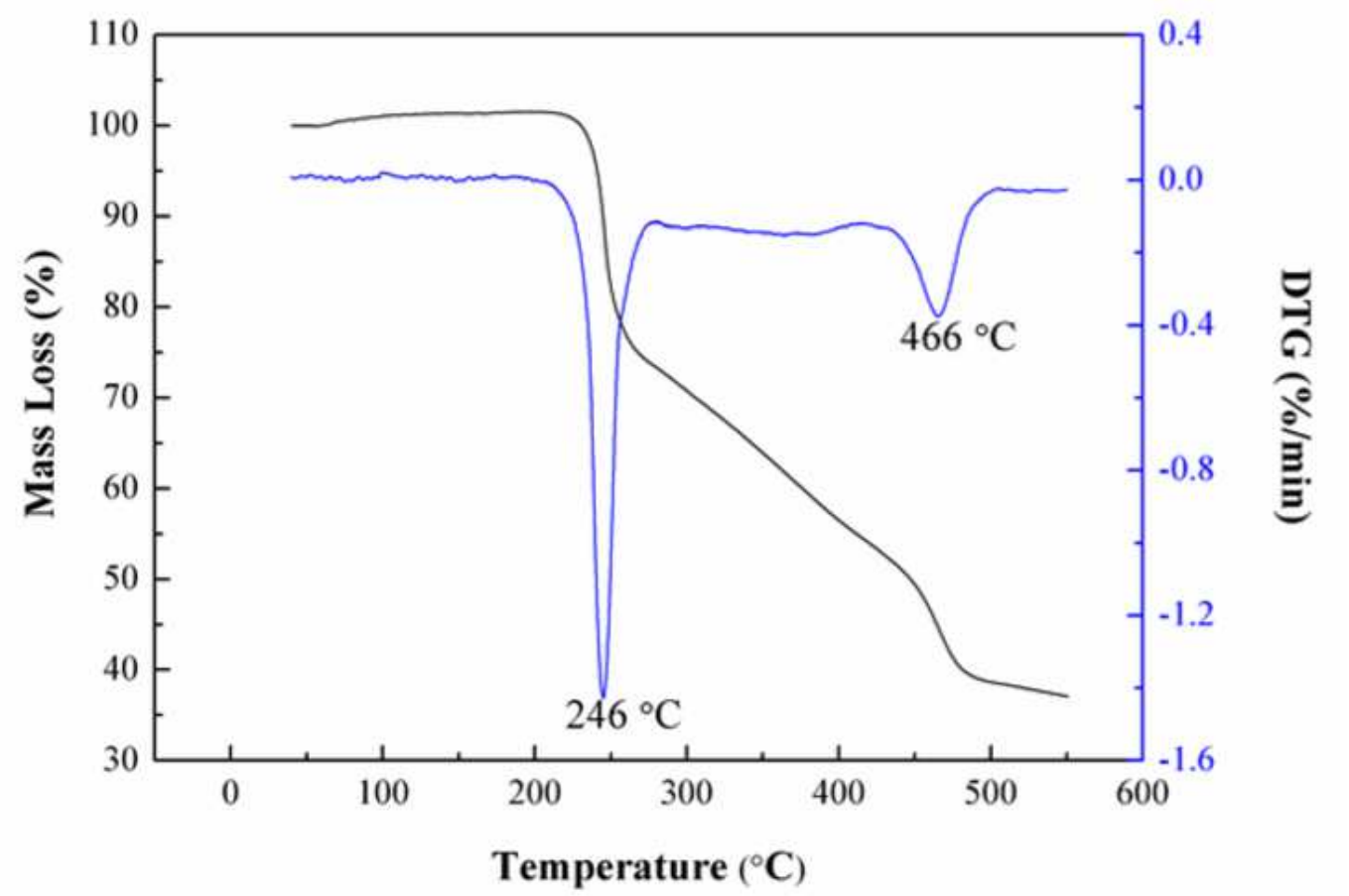

Figure 7

TG/DTG curves of PBFMO-b-GAP copolyurethane.

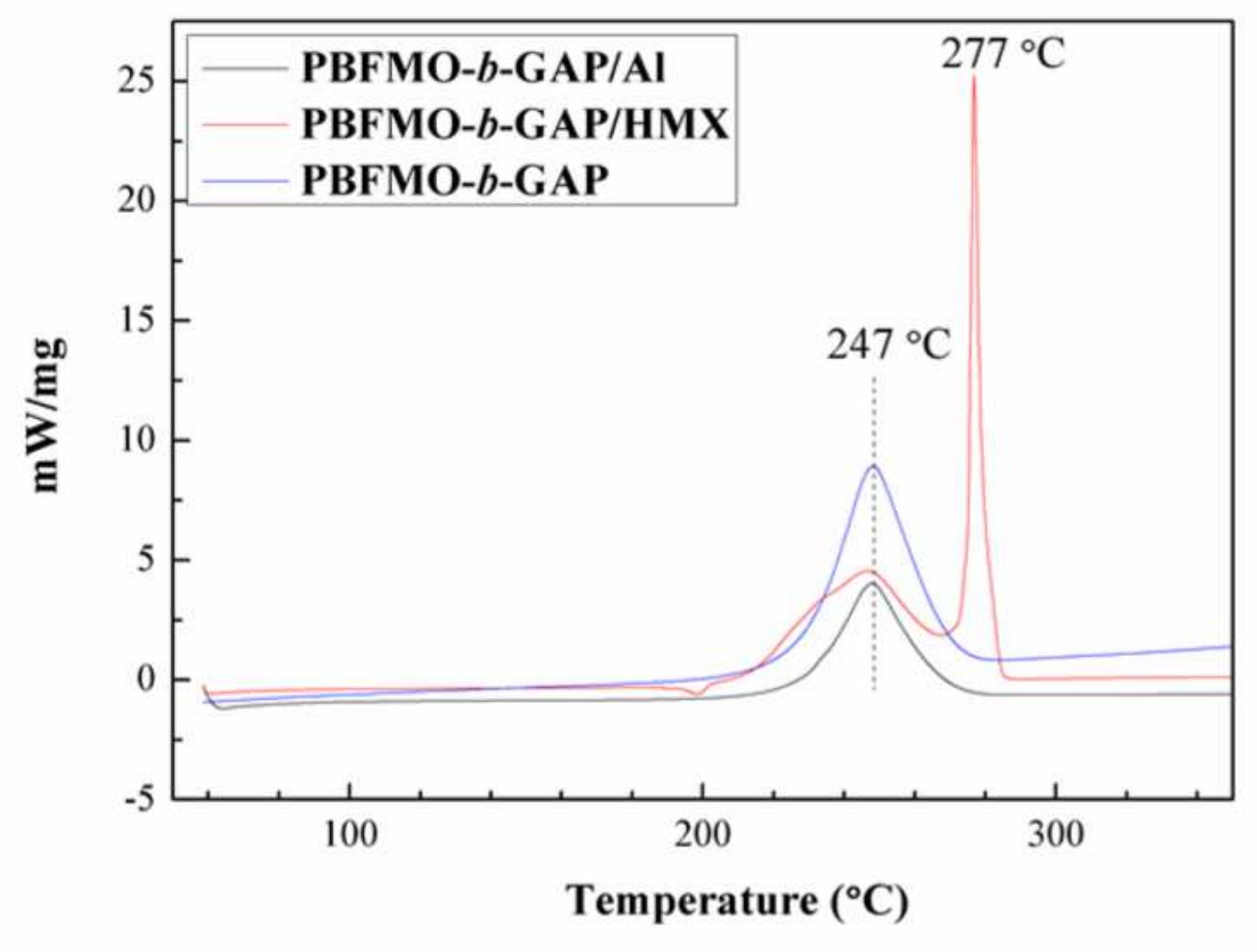

Figure 8

DSC curves of PBFMO-b-GAP, PBFMO-b-GAP/HMX complex and PBFMO-b-GAP/Al complex.

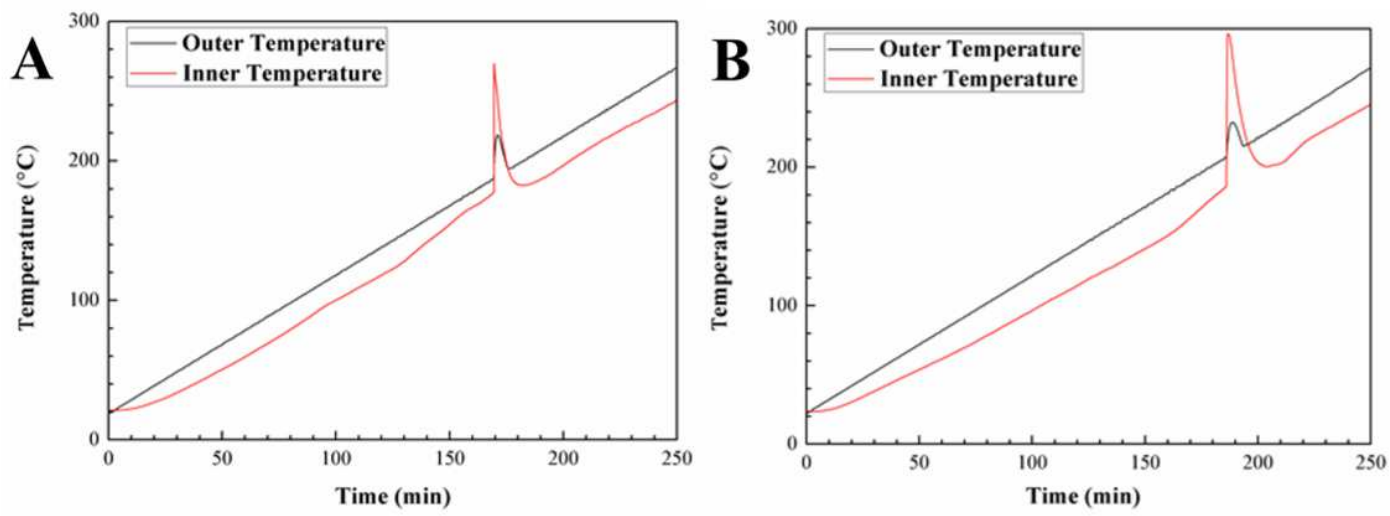

Figure 9

Cook-off curves of GAP-ETPE/Al (A) and PBFMO-b-GAP/Al (B)

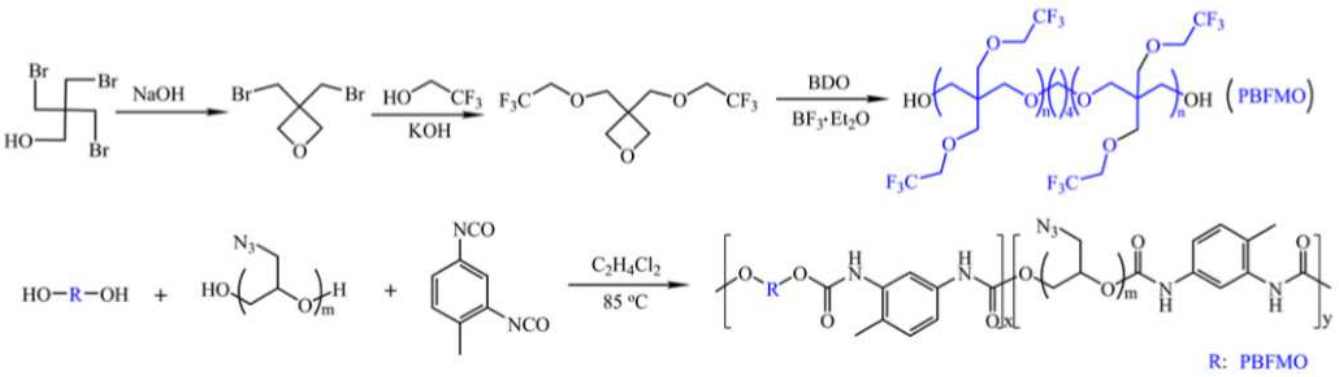

Figure 10

The synthesis route of PBFMO-b-GAP copolyurethane

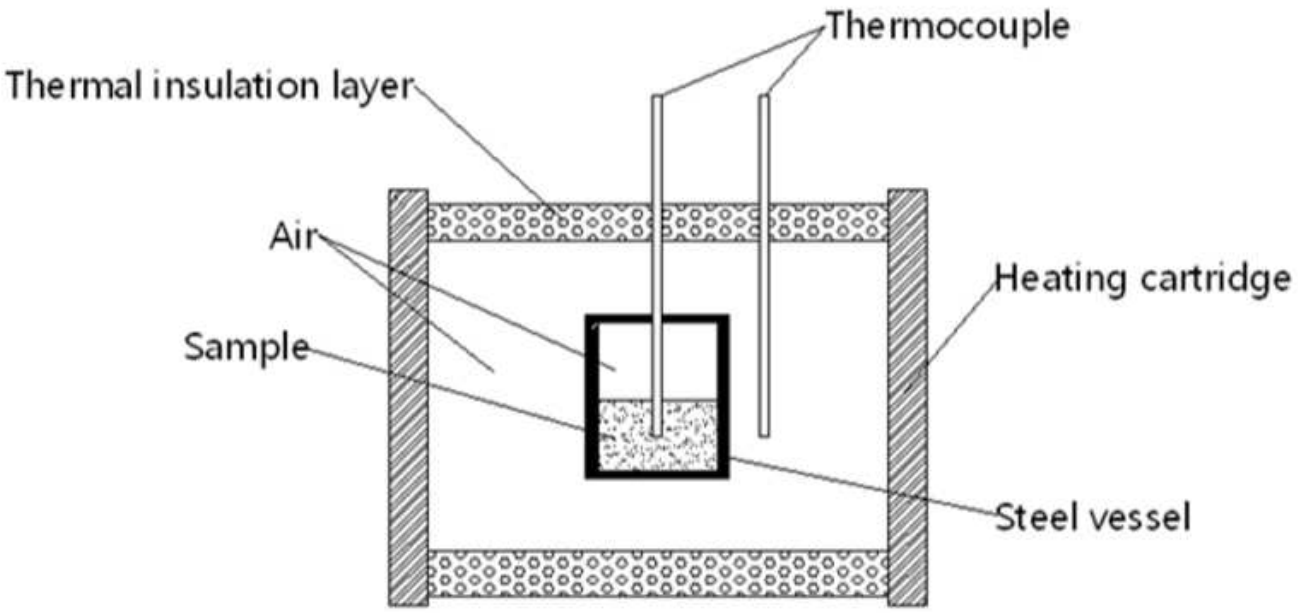

Figure 11

Schematic geometry of cook-off test